RESEARCH ARTICLE

Comparison between Computer Tomography and Magnetic Resonance Imaging in the Diagnosis of Small Hepatocellular Carcinoma

Korn Lertpipopmetha[1], Teeravut Tubtawee[2], Teerha Piratvisuth[1], Naichaya Chamroonkul[1]*

Abstract

Background: Hepatocellular carcinomas (HCCs) less than 2 cm in diameter generally demonstrate a good outcome after curative therapy. However, the diagnosis of small HCC can be problematic and requires one or more dynamic imaging modalities. This study aimed to compare the sensitivity and agreement between CT and MRI for the diagnosis of small HCCs. **Methods:** CT and/or MRI scans of HCCs (1-2 cm) diagnosed by histopathology or typical vascular pattern according to the 2005 AASLD criteria were blindly reviewed by an abdominal radiologist. The reports were defined as conclusive/typical when arterial enhancement and washout during the portal/delayed phases were observed and as inconclusive when typical vascular patterns were not observed. The sensitivity and Cohen's kappa (k) for agreement were calculated. **Results:** In 27 patients, 27 HCC nodules (1-2 cm) were included. Diagnosis with a single-imaging modality (CT or MRI) was 81 % versus 48 % ($p = 0.01$). The CT sensitivity was significantly higher than MRI (78 % versus 52 %, $p = 0.04$). Among 27 nodules that underwent both CT and MRI, a discordance in typical enhancement patterns was found ($k = 0.319$, $p = 0.05$). In cases with inconclusive CT results, MRI gave only an additional 3.7 % sensitivity to reach a diagnosis. In contrast, further CT imaging following inconclusive MRI results gave an additional 29.6 % sensitivity.**Conclusions:** A single typical imaging modality is sufficient to diagnose small HCCs. Compared with MRI, multiphasic CT has a higher sensitivity. The limitations of MRI could be explained by the greater need for patient cooperation and the types of MRI contrast agent.

Keywords: Small hepatocellular carcinoma - computed tomography - magnetic resonance imaging - sensitivity

Asian Pac J Cancer Prev, **17 (11)**, 4805-4811

Introduction

Hepatocellular carcinoma (HCC) is one of the most common cancers worldwide, especially in Southeast Asia, where chronic hepatitis B infection has a high prevalence (International Agency for Research on Cancer, 1987; Munoz et al., 1989; Bosch et al., 1991; Okuda et al., 1992). In the era of regular surveillance programs for all at-risk populations, the prevalence of newly detected small tumors less than 2 cm in diameter increased to 30 % in Japan, whereas the prevalence was less than 5 % in the early nineties in Europe (European Association For The Study Of The Liver, 2012). Nevertheless, the diagnosis of small HCC (1-2 cm) could be difficult because of the lack of typical vascular patterns on dynamic imaging (Bosch et al., 1991; Okuda et al., 1992; Bosch et al., 1999; Chen et al., 2010), and the diagnosis often requires the use of more than one imaging modality (Bruix et al., 2011; Forner et al., 2012).

Recently published guidelines by the American Association for the Study of Liver Diseases (AASLD) and the European Association for the Study of the Liver (EASL) proposed a diagnostic algorithm for HCC nodules 1-2 cm in diameter (Bruix et al., 2011; European Association For The Study Of The Liver, 2012). The guidelines included the detection of arterial hypervascularity and portal or delayed venous washout in only one dynamic radiological procedure, either multidetector computed tomography (MDCT) or dynamic magnetic resonance imaging (MRI). When these features are not present, either a second contrast-enhanced imaging study or image-guided biopsy is recommended.

The most suitable initial imaging technique (CT or MRI) and the sequential diagnostic strategy that gives the best diagnostic accuracy in small HCC are still in consideration due to a variety of diagnostic sensitivities based on previous studies (Rode et al., 2001; Bolondi et al., 2005; Forner et al., 2008; Yu et al., 2008; Sangiovanni et al., 2010; Kim et al., 2011; Yu et al., 2011; Serste et al., 2012; Park et al., 2014). One study found that the best diagnostic strategy was a sequential imaging study (inconclusive MRI result followed by CT scan) with

*[1]Department of Internal Medicine, [2]Department of Radiology, Faculty of Medicine Songklanagarind Hospital, Prince of Songkla University,15 Kanjanavanich Rd., Hatyai, Songkhla, Thailand . *For Correspondence: naichaya@gmail.com*

a sensitivity of 74 % instead of a second concomitant imaging study (combination of CT and MRI) (Khalili et al., 2011). However, one could argue that such a strategy would leave some underdiagnosed HCC in 26 % of the cases and was not cost effective (Sangiovanni et al., 2010).

The aim of this study was to compare the sensitivity and agreement between multidetector computed tomography (MDCT) and dynamic magnetic resonance imaging (MRI) for the diagnosis of small hepatocellular carcinoma (1-2 cm).

Material and Methods

Study population

This study was a retrospective analysis that focused on patients under the care of the Department of Medicine, Faculty of Medicine at Songklanagarind Hospital, which is the largest tertiary referral university hospital in the southern part of Thailand, between 1 March 2008 and 1 March 2014. The study was approved by the Institutional Review Board of the Faculty of Medicine, Prince of Songkla University. The diagnosis of cirrhosis was based on either histopathology or a combination of physical examination, laboratory tests, and imaging data. The diagnosis of HCC was based on histopathology or the 2005 AASLD diagnostic criteria, in which a coincidental typical vascular pattern (i.e. enhancement during the hepatic arterial phase and washout during the hepatic venous and/or delayed phase) is observed with both imaging techniques (CT and MRI).

The patient inclusion criteria were as follows: 1) diameter of HCC between 1 and 2 cm; 2) both CT and MRI were available and showed satisfactory nodule visibility for review; 3) patients at risk (i.e. cirrhosis from any cause); and 4) age > 18 years. The demographic and clinical characteristics, including age, gender, etiology of cirrhosis, level of serum alpha-fetoprotein and baseline liver function laboratory results were documented for each patient.

Imaging technique

MDCT

Helical multidetector quadruple-phase CT was performed using a 64-section scanner (Philips Brilliance, Royal Philips Electronics, Netherlands) with a collimation of 64 x 0.625 mm. Images with an effective section thickness of 3.0 mm were reconstructed every 2 mm. The contrast-enhanced liver images were obtained after a bolus intravenous injection of 2.0 mL/kg of a nonionic contrast agent (Iomeron 350, Bracco or Ultravist 370, Bayer) at a rate of 3-3.5 mL/s through an 18-20 gauge intravenous catheter, followed by a flush of 50 mL of saline administered at the same injection site. The start of the scans was triggered according to a test tracker positioned over the abdominal aorta. The scans started 18 s (late arterial phase) after reaching the trigger threshold (150 HU) in the aorta, 70 s (portal venous phase) and 180 s (delayed phase).

MRI

MRI was performed with 1.5 T scanners (Vision, Siemens, Germany [from November 1995 to June 2012] and Ingenia, Philips, Netherlands [from July 2012]) using a body phased-array multicoil for signal detection. All patients underwent transverse T1-weighted and T2-weighted MRI and multiphasic contrast enhanced dynamic 3-dimensional MRI of the whole liver with fat suppression.

The imaging protocol included axial pre-contrast images acquired with a T2-weighted fast-spin echo sequence (TR/TE = 4009/80 ms, section thickness 5–7 mm) and T1-weighted in-phase and out-of-phase gradient-recalled-echo (GRE) sequences (TR/TE = 6.5/2.3-4.6 ms, section thickness, 2–3 mm). Dynamic studies were performed with three-dimensional T1-weighted GRE sequence (Vision, Siemens: TR/TE = 5.2/2.6 ms; Flip angle 20°; section thickness 3 mm and Ingenia, Philips: TR/TE = 3.9/1.85 ms; Flip angle 10°; section thickness 2-3 mm). The contrast agents were varyingly administered according time deference and included Gadovist® Bayer Germany, gadopentetate dimeglumine 0.5 mmol/mL; Magnevist® Bayer Germany or MultiHance® Bracco Italy, gadoteric acid 0.5 mmol/mL; Dotarem® Guerbet France, and gadoterate meglumine 0.5 mmol/mL. The contrast was injected manually at a dose of 0.2 mL/kg body weight at a rate of 2 mL/s through a 20-23-gauge intravenous catheter. The arterial phase, portal venous and delayed venous phase images were acquired at 30, 60 and 180 s from the start of contrast injection, respectively. The additional hepatobiliary phase was not used in our study.

Imaging analysis

The images were read blindly by a board certified radiologist (T.T.) with more than 5 years of experience in liver imaging who was unaware of the patient's profile, treatment, and other contrast techniques. For each imaging study, the number, size, location, and vascular pattern of the lesions were detected and analyzed.

Vascular pattern was qualified as ''conclusive'' for HCC if contrast washout occurred, defined as the presence of hypervascularity during the arterial phase followed up by a hypodense/hypointense appearance in later phases defining washout. Nodules in which an enhancement was found during the arterial phase with- out washout were qualified as ''suspicious.''

The conclusive radiological pattern of HCC for both imaging techniques (CT or MRI) was arterial hypervascularization followed by portal/venous or delay contrast washout of the nodule. Arterial hypervascularization was seen as increased contrast enhancement of the nodule (hyperdensity on CT and hyperintensity on MRI) taking place during the arterial phase of the examination as compared with the surrounding liver parenchyma. Portal/venous contrast washout was seen as a hypoenhanced pattern of the nodule (hypodensity on CT and hypointensity on MRI) with respect to the surrounding liver parenchyma taking place during the portal/venous or delay phase. Nodules with only arterial enhancement without venous washout were classified as suspicious findings. The remaining nodules with negative arterial enhancement were defined as non-diagnostic nodules. For MRI, T1-weighted, T2-weighted

and DWI data were not included for the diagnostic vascular analysis.

Liver histology

Ultrasound-guided biopsy was performed using Quick-Core® biopsy needles before January 2014 (COOK Medical, Bloomington, USA) and semi-automatic biopsy needles from January 2014 (GEOTEK Medical, Ankara, Turkey). The specimens were routinely processed and stained with hematoxylin and eosin by the Masson trichrome method.

Statistical analysis

The sensitivity and inter-modality agreement were calculated for the nodules that underwent both MDCT and dynamic MRI. Cohen's kappa statistic (k) for the inter-modality agreement was calculated. Kappa values less than 0.2 indicated positive but poor agreement, 0.2–0.4 indicated fair agreement, 0.4–0.6 indicated moderate agreement, 0.6–0.8 indicated good agreement, and greater than 0.81 indicated excellent agreement. Associations between the continuous and categorical variables were analyzed using the Mann Whitney U-test and the chi-square test or Fisher's exact test, respectively. Statistical significance was defined as a p value less than 0.05. The statistical analyses were performed using the SPSS 11.5 software package (SPSS Inc., Chicago, IL, USA).

Results

During the study period, 67 patients from the data registry met the criteria for diagnosis of a 1-2 cm HCC. The thirty-one cases were excluded according to utility of single imaging for diagnosis and proceeding to definite treatment. Thirty-six small HCC patients underwent

Table 1. Baseline Characteristics of All Patients

	All	Histopathology
Number of nodules	27.0	14
Age mean ± SD (range)	61 ± 11.7	63 ± 10.1
	(37-82)	(49-82)
Sex, Male (%)	21.0 (77.8)	9.0 (64.3)
Population at risk of Cirrhosis (%)	27.0 (100.0)	14.0 (100.0)
Etiology of cirrhosis (%)		
HBV	11.0 (40.7)	5.0 (35.7)
HCV with co-infection	5.0 (18.5)	3.0 (21.4)
Alcohol	8.0 (29.6)	4.0 (28.6)
Others[a]	3.0 (11.1)	2.0 (14.3)
Child-Pugh class (%)		
A	22.0 (81.5)	12.0 (85.7)
B	5.0 (18.5)	2.0 (14.3)
Median AFP, ng/mL (range)	19.0 (2.0-140.0)	14.0 (2.0-86.0)
USG surveillance (%)	25.0 (92.6)	13.0 (92.9)
Method for pathologic confirmation (%)		
FNB	12.0 (44.4)	12.0 (85.7)
Surgery	2.0 (7.4)	2.0 (14.3)
Treatment (%)		
Intervention[b]	25.0 (92.6)	12.0 (85.7)
Surgery	2.0 (7.4)	2.0 (14.3)
Laboratory investigation (range)		
INR	1.1 (0.9-1.5)	1.1 (0.9-1.3)
Platelet count (103/µl)	103.0 (30.0-185.0)	103.0 (30.0-185.0)
TB (mg/dl)	1.2 (0.3-11.1)	1.2 (0.4-5.1)
Albumin (g/dl)	3.7 (2.4-4.9)	3.8 (2.8-4.8)
AST (U/L)	51.0 (22.0-120.0)	44.0 (22.0-120.0)
ALT (U/L)	34.0 (13.0-95.0)	29.0 (14.0-59.0)
ALP (U/L)	109.0 (55.0-220.0)	113.0 (60.0-163.0)
Cr (mg/dl)	1.0 (0.6-1.8)	1.0 (0.6-1.8)
Duration to diagnosis[c], days (range)	59.0 (1.0-357.0)	60.0 (16.0-273.0)
Mean size of the maximal diameter of nodule, mm (range)	16.0 (10.0-20.0)	17.0 (12.0-20.0)

[a], Consisted of cryptogenic (N = 2, 7.4 %), autoimmune hepatitis (N = 1, 1.7 %); [b], Consisted of PEI (N = 17, 63 %), RFA (N = 1, 3.7 %), TOCE (N = 7, 25.9 %); [c],The median of the data set.

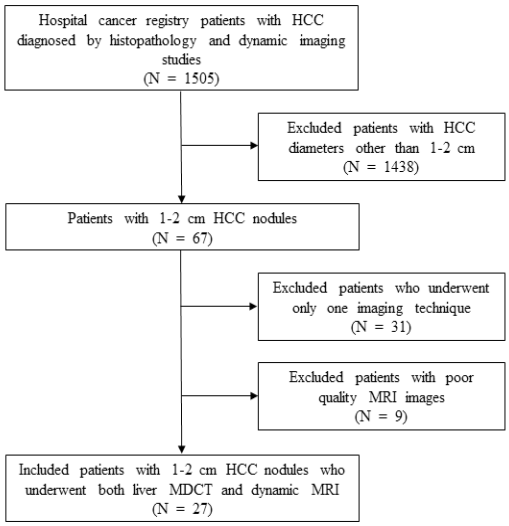

Figure 1. Schematic Outline of the Study Process

both CT and MRI, and nine were excluded because of poor MRI quality. We enrolled 27 consecutive patients, including 21 men and 6 women with a mean age of 61 years (range, 37–82 years). The mean size of the 27 HCC nodules was 16 mm (range, 10-20 mm) and consisted of 14 pathologically confirmed nodules. Figure 1 illustrates the outline of the study enrollment.

Cirrhosis was diagnosed in all patients. Underlying liver cirrhosis was associated with viral hepatitis B in 11 patients, viral hepatitis C in 4 patients, hepatitis B virus and hepatitis C virus co-infection in 1 patient, and alcoholic cirrhosis in 8 patients. The other causes of cirrhosis consisted of cryptogenic cirrhosis in 2 patients and autoimmune hepatitis in 1 patient. Based on the Child-Pugh classification, 22 patients were classified as Child-Pugh class A, and the remaining 5 patients were class B. The demographic, baseline clinical, and biochemical characteristics of the study patients are summarized in Table 1.

There were no significant differences in the baseline clinical or biochemical characteristics between the

Table 2. Frequency of Vascular Pattern between Types of Imaging for 1-2 cm HCC

		All nodules N (%)
MDCT (N = 27)	Conclusive	21 (78)
	Suspicious	3 (11)
	Non-diagnostic	3 (11)
MRI (N = 27)	Conclusive	14 (52)
	Suspicious	6 (22)
	Non-diagnostic	7 (26)
	T1W (hyper/hypo/isointensity)	11/11/5 (41/41/18)
	T2W (hyper/hypo/isointensity)	19/3/5 (70/11/19)

Conclusive, refers to arterial enhancement and washout during portal or delayed phases; Suspicious, refers to arterial enhancement without washout during portal or delayed phases; Non-diagnostic, refers to no arterial enhancement.

Table 3. Agreement and Disagreement between Types of Imaging for 1-2 cm HCC

	Arterial enhancement	Portovenous/Delay phase washout
Agreement		
MDCT (C) MRI (C)	19 (70.4)	13 (48.1)
MDCT (I) MRI (I)	2 (7.4)	3 (11.1)
Disagreement		
MDCT (C) MRI (I)	5 (18.5)	10 (37.0)
MDCT (I) MRI (C)	1 (3.7)	1 (3.7)
Kappa Value	0.289	0.163
P value	0.088	0.244

Note, Numbers are the number of lesions (%); (C), Presence of arterial enhancement and presence of washout; conclusive enhancement pattern; (I), Presence of arterial enhancement without washout or absence of arterial enhancement; inconclusive enhancement pattern.

histopathologically and non-histopathologically diagnosed groups. The median duration between the first and second imaging sessions was 32 days (min-max, 4-125 days). The frequency vascular pattern of CT and MRI is shown in Table 2. On CT, the nodules were of the conclusive pattern (i.e. defined as arterial enhancement and washout during the portal or delayed phases) in 21 of 27 cases, whereas the nodules were of the conclusive pattern in 14 of 27 cases on MRI. Suspicious patterns of nodules on CT and MRI were observed in 11 % and 22 % of cases, respectively. According to the signal intensity on standard MRI sequences, hyperintensity and hypointensity of nodules on T1-weighted images occurred in 41 % and 41 %, respectively, whereas they were 70 % and 11 % on T2-weighted images, respectively.

Conclusive findings for the diagnosis of HCC were detected in both imaging modalities in 56 % (15/27) of the HCC nodules. The inter-modality agreement for the assessment of a conclusive or inconclusive tumor enhancement pattern was 67 % (18/27) ($k = 0.319$, $p = 0.05$). Arterial enhancement on both imaging techniques was detected in 70.4 % (19/27) of the HCC nodules. Agreement for the detection of the presence or absence of arterial enhancement was 78 % (21/27) ($k = 0.289$, $p = 0.088$). A tumor washout pattern on both imaging techniques was detected in 48 % (13/27) of the HCC nodules. Agreement for the detection of the presence or absence of portovenous/delay washout was 59 % (16/27) ($k = 0.163$, $p = 0.244$). The agreement and disagreement of specific HCC enhancement patterns of CT and MRI are shown in Table 3.

The diagnostic sensitivity of CT and MRI is shown in Table 4. The sensitivity to diagnose HCC was 78 % on CT and 52% on MRI ($p = 0.04$), respectively. In the histopathology proven group, the CT scan also had a higher sensitivity than MRI (86 % versus 43 %, $p = 0.02$). The sensitivity of a conclusive pattern to diagnose HCC on at least one of the two imaging studies was 81 %, whereas the sensitivity was 48 % on both imaging studies ($p = 0.01$).

In patients with inconclusive CT results, proceeding to MRI gave only an additional 3.7 % sensitivity to

Table 4. Sensitivity between Types of Imaging for Diagnosis of 1-2 cm HCC

	All nodules underwent both CT and MRI (N = 27)		Histopathology group (N = 14)	
	Sensitivity (%)	p value	Sensitivity (%)	p value
MDCT	78		86	
MRI	52	0.04	43	0.02
MDCT or MRI	81		86	
MDCT and MRI	48	0.01	43	0.02

Conclusive (typical), refers to arterial enhancement and washout during portal or delayed phases; Inconclusive (atypical), refers to arterial enhancement without washout during portal or delayed phases or no arterial enhancement.

reach a diagnosis. In cases of inconclusive MRI results, a further CT gave an additional 29.6 % sensitivity to reach a diagnosis.

Discussion

Our results confirmed that CT or MRI yielded a better sensitivity rate of 81 % for HCC diagnosis of 1-2 cm nodules compared with a combination of CT and MRI, in which case the sensitivity dropped to 48 %. This finding supported previous studies (Forner et al., 2008; Sangiovanni et al., 2010; Leoni et al., 2010; Khalili et al., 2011; Serste et al., 2012; Furlan et al., 2012) that reported that the sensitivity of coincidental conclusive findings in both imaging techniques was less than that of a single imaging technique.

The study results showed fair agreement (67 % (k = 0.319)) between the CT and MRI findings for an illustration of typical tumor enhancement pattern of 1-2 cm HCC nodules. This finding is consistent with previous studies (Leoni et al., 2010; Sangiovanni et al., 2010) found that the tumor enhancement pattern (typical or atypical) was concomitantly detected in only 64 % and 59 % of 10–20 mm HCC nodules, respectively. However, another recent study (Furlan et al., 2012) showed good agreement between CT and MRI (81 %, k = 0.607).

Our study showed a discordance between CT and MRI imaging because the portovenous/delay washout (59 %, k = 0.16) appeared to be more than that of arterial enhancement (78 %, k = 0.29). The resolution of tumor washout was affected by many factors, such as the degree of (Jang et al., 2007; Liu et al., 2007; Park et al., 2014) histological differentiation, the timing sequence of the tumor washout phase, the degree of fibrotic liver parenchyma (Vignaux et al., 1999; Yu et al., 2008), contrast agent diffusion, and fat in the lesions (Wilson et al., 2007; Khan et al., 2010).

Based on a single modality for HCC diagnosis of 1-2 cm nodules, our results showed that CT had a higher sensitivity than MRI (78 % versus 52 %), which was different from the findings of some previous studies (Leoni et al., 2010; Hwang et al., 2012; Serste et al., 2012; Park et al., 2014) that reported a tendency of MRI to have a higher sensitivity than a CT scan in the diagnosis of small HCC less than 2 cm in diameter (44-74 % on CT and 42-82 % on MRI) (Rode et al., 2001; Bolondi et al., 2005; Forner et al., 2008; Yu et al., 2008; Sangiovanni et al., 2010; Kim et al., 2011; Yu et al., 2011; Serste et al., 2012; Park et al., 2014). The recent study (Sangiovanni et al., 2010) showed that the sensitivity and accuracy of CT scan for HCC diagnosis of 1-2 cm nodules was equal to MRI (44 % versus 44 % and 65 % versus 66 %).

The explanations for the higher sensitivity of the CT scan than MRI in our study might be because more patient cooperation is needed in the MRI room than in a CT scan to achieve a high resolution and the fewest number of imaging artifacts. Although there were no reported studies on the correlation between the sensitivity of liver MRI and patient cooperation, two studies of coronary MRI suggested that poor patient cooperation played an important role in poor imaging resolution and low sensitivity of the technique (Danias et al., 1998; Nikolaou et al., 2002). Furthermore, the utility of different contrast agents across the studies' time was the factor that might affect the result. A recent meta-analysis (Kierans et al., 2016) showed that the use of gadoxetate disodium as a MRI contrast agent was independently associated with a higher sensitivity of HCC diagnosis in small nodules. Finally, most of the studies in the meta-analysis (Kierans et al., 2016) that showed a higher sensitivity of MRI performed hepatobiliary phase imaging, which could enhance the test sensitivity but also adds expenses to the test; therefore, the cost effectiveness analysis of first-line imaging for diagnosis of small HCC should be examined in a future study.

Adding a sequential MRI to the CT scan only resulted in a diagnosis in an additional 3.7 %. We suggest proceeding with a liver biopsy if the CT shows an inconclusive result after seriously considering the procedure risks.

Our study had several limitations. First, the study was performed in a single center, and its retrospective nature possibly introduced a selection bias. Second, not all tumors were pathologically confirmed. Nevertheless, we attempted to confute this effect by a subgroup analysis performed only in the histopathology group, which still showed that CT had a higher sensitivity than MRI. Moreover, acquiring pathological confirmation of all hepatic nodules less than 2 cm in size in a cirrhotic liver would not be practical in clinical settings. Third, we excluded more than 50 % of patients who underwent single imaging and proceeded to HCC treatment; however, we also analyzed the sensitivity of CT and MRI in this group. The results confirmed a higher sensitivity for CT than MRI. Finally, our study included only HCC; therefore, there might have been a potential bias for the radiologist when interpreting the CT and MRI findings.

Multiphasic CT has a higher sensitivity than MRI for the diagnosis of small HCC less than 2 cm in size. The need to have greater patient cooperation and the type of MRI contrast agents could explain the limitations of MRI

in our study. A single typical imaging modality is sufficient to diagnose small HCC nodules in over 80 % of patients. We propose a CT scan as the first imaging modality and then proceeding to perform an ultrasound-guided liver biopsy in cases of inconclusive imaging.

Declarations

Abbreviations

HCC: Hepatocellular carcinoma; AASLD: American Association for the Study of Liver Diseases; CT: Computed tomography; MDCT: Multidetector computed tomography; MRI: Magnetic resonance imaging; HU: Hounsfield Unit; GRE: Gradient-recalled-echo; TR: repetition time; TE: echo time; k: Cohen's kappa statistic; HBV: Hepatitis B virus; HCV: Hepatitis C virus; PEI: Percutaneous ethanol injection; RFA: Radiofrequency ablation; TOCE: Transarterial Oily-chemoembolization.

Ethics approval

This study was approved by the Ethics Committee, Faculty of Medicine, Prince of Songkla University (EC reference number: 56-158-14-4-3).

Consent for publication

Not applicable

Availability of data and materials

The dataset supporting the conclusions of this article is included within the article and the additional file.

Additional files

Additional file 1: General dataset.

Competing interests

All of the authors declare no competing interests.

Funding

The role of the funding body in the design of the study and collection, analysis, and interpretation of data and in writing the manuscript were supported by the Faculty of Medicine Prince of Songkla University Hospital Research Foundation.

Authors' Contributions

KL was responsible for the data collection and analysis and drafting of the manuscript. KL and TP supervised all processes of the study and the writing of the manuscript. TT was the radiologist who performed all imaging interpretations and helped to design the study. NC was KL's major advisor who was responsible for the initiation and execution of the project and for critical revision of the manuscript. All authors read and approved the final manuscript.

Acknowledgements

The authors would like to thank Assoc. Prof. Supamai Soonthornpun, Dr. Pimsiri Sripongpun, Dr. Treechada Wisaratapong for suggestions regarding the composition of the manuscript.

References

Bolondi L, Gaiani S, Celli N, et al (2005). Characterization of small nodules in cirrhosis by assessment of vascularity: the problem of hypovascular hepatocellular carcinoma. *Hepatology*, **42**, 27-34.

Bosch FX, Munoz N (1991). Hepatocellular carcinoma in the world: Epidemiologic questions. In 'Etiology, Pathology and Treatment of Hepatocellular Carcinoma in America', Eds Tabor E, DiBisceglie AM and Purcell RH. Advances in Applied Technology Series, Gulf, Houston p 35.

Bosch FX, Ribes J, Borras J (1999). Epidemiology of primary liver cancer. *Semin Liver Dis*, **19**, 271-85.

Bruix J, Sherman M (2011). Management of hepatocellular carcinoma: an update. *Hepatology*, **53**, 1020-2.

Chen JD, Yang HI, Iloeje UH, et al (2010). Carriers of inactive hepatitis B virus are still at risk for hepatocellular carcinoma and liver-related death. *Gastroenterology*, **138**, 1747-54.

Danias PG, Edelman RR, Manning WJ (1998). Coronary MR angiography. *Cardiol clin*, **16**, 207-25.

European Association For The Study Of The Liver (2012). EASL-EORTC clinical practice guidelines: management of hepatocellular carcinoma. *J Hepatol,* **56**, 908-43.

Forner A, Llovet JM, Bruix J (2012). Hepatocellular carcinoma. *Lancet*, **379**, 1245-55.

Forner A, Vilana R, Ayuso C, et al (2008). Diagnosis of hepatic nodules 20 mm or smaller in cirrhosis: Prospective validation of the noninvasive diagnostic criteria for hepatocellular carcinoma. *Hepatology*, **47,** 97-104.

Furlan A, Marin D, Cabassa P, et al (2012). Enhancement pattern of small hepatocellular carcinoma (HCC) at contrast-enhanced US (CEUS), MDCT, and MRI: intermodality agreement and comparison of diagnostic sensitivity between 2005 and 2010 American Association for the Study of Liver Diseases (AASLD) guidelines. *Eur J Radiol*, **81**, 2099-105.

Hwang J, Kim SH, Lee MW, et al (2012). Small (</= 2 cm) hepatocellular carcinoma in patients with chronic liver disease: comparison of gadoxetic acid-enhanced 3.0 T MRI and multiphasic 64-multirow detector CT. *Br J Radiol*, **85**, 314-22.

International Agency for Research on Cancer (1987). Cancer incidence in five continents, Volume V, Eds Muir C, Waterhouse J, Mack T, et al. IARC Scientific Publication, Lyon pp 1-970 Number 88.

Jang HJ, Kim TK, Burns PN, et al (2007). Enhancement patterns of hepatocellular carcinoma at contrast-enhanced US: comparison with histologic differentiation. *Radiology*, **244**, 898-906.

Khalili K, Kim TK, Jang HJ, et al (2011). Optimization of imaging diagnosis of 1-2 cm hepatocellular carcinoma: an analysis of diagnostic performance and resource utilization. *J Hepatol*, **54**, 723-8.

Khan AS, Hussain HK, Johnson TD, et al (2010). Value of delayed hypointensity and delayed enhancing rim in magnetic resonance imaging diagnosis of small hepatocellular carcinoma in the cirrhotic liver. *J Magn Reson*, **32**, 360-6.

Kierans AS, Kang SK, Rosenkrantz AB (2016). The Diagnostic Performance of Dynamic Contrast-enhanced MR Imaging for Detection of Small Hepatocellular Carcinoma Measuring Up to 2 cm: A Meta-Analysis. *Radiology*, **278**, 82-94.

Kim TK, Lee KH, Jang HJ, et al (2011). Analysis of gadobenate dimeglumine-enhanced MR findings for characterizing small (1-2 cm) hepatic nodules in patients at high risk for hepatocellular carcinoma. *Radiology*, **259**, 730-8.

Leoni S, Piscaglia F, Golfieri R, et al (2010). The impact of vascular and nonvascular findings on the noninvasive

diagnosis of small hepatocellular carcinoma based on the EASL and AASLD criteria. *Am J Gastroenterol*, **105**, 599-609.

Liu GJ, Xu HX, Lu MD, et al (2007). Correlation between enhancement pattern of hepatocellular carcinoma on real-time contrast-enhanced ultrasound and tumour cellular differentiation on histopathology. Br J Radiol, **80**, 321-30.

Munoz N, Bosch X (1989). Epidemiology of hepatocellular carcinoma. In 'Neoplasms of the Liver', Eds Okuda K and Ishak KG. Springer, Tokyo p 3.

Nikolaou K, Huber A, Knez A, et al (2002). Intraindividual comparison of contrast-enhanced electron-beam computed tomography and navigator-echo-based magnetic resonance imaging for noninvasive coronary artery angiography. *Eur Radiol*, **12**, 1663-71.

Okuda K (1992). Epidemiology of primary liver cancer. In 'Primary Liver Cancer in Japan', Ed Tobe T. Springer-Verlag, Tokyo p 3.

Park VY, Choi JY, Chung YE, et al (2014). Dynamic enhancement pattern of HCC smaller than 3 cm in diameter on gadoxetic acid-enhanced MRI: comparison with multiphasic MDCT. *Liver Int*, **34**, 1593-602.

Rode A, Bancel B, Douek P, et al (2001). Small nodule detection in cirrhotic livers: evaluation with US, spiral CT, and MRI and correlation with pathologic examination of explanted liver. *J Comput Assist Tomogr,* **25**, 327-36.

Sangiovanni A, Manini MA, Iavarone M, et al (2010). The diagnostic and economic impact of contrast imaging techniques in the diagnosis of small hepatocellular carcinoma in cirrhosis. *Gut*, **59**, 638-44.

Serste T, Barrau V, Ozenne V, et al (2012). Accuracy and disagreement of computed tomography and magnetic resonance imaging for the diagnosis of small hepatocellular carcinoma and dysplastic nodules: role of biopsy. *Hepatology*, **55**, 800-6.

Vignaux O, Legmann P, Coste J, et al (1999). Cirrhotic liver enhancement on dual-phase helical CT: comparison with noncirrhotic livers in 146 patients. *Am J Roentgenol*, **173**, 1193-7.

Wilson SR, Kim TK, Jang HJ, et al (2007). Enhancement patterns of focal liver masses: discordance between contrast-enhanced sonography and contrast-enhanced CT and MRI. *Am J Roentgenol*, **189**, W7-W12

Yu JS, Lee JH, Chung JJ, et al (2008). Small hypervascular hepatocellular carcinoma: limited value of portal and delayed phases on dynamic magnetic resonance imaging. *Acta Radiol*, **49**, 735-43.

Yu NC, Chaudhari V, Raman SS, et al (2011). CT and MRI improve detection of hepatocellular carcinoma, compared with ultrasound alone, in patients with cirrhosis. *Clin Gastroenterol Hepatol*, **9**, 161-7.